

The Effect of Temperature on The Efficiency of The Reduction of Graphene Oxide

Kyeong-Won Park

Abstract— Comparative spectroscopic and microscopic analyses of the oxygen content in oxygen-containing functional groups for graphene oxide and its reduced form are reported. The graphene oxide prepared by Hummers method using graphite flakes was used as a starting material. Reduced graphene oxide was obtained through the reduction of the graphene oxide sheets with hydrazine hydrate at room temperature and 98 °C. The comparison of the oxygen content and functionality before and after the reduction of graphene oxides at different temperatures were investigated by XRD, AFM, SEM, TEM, FT-IR, XPS, and Raman spectroscopy. The reduced graphene oxides showed much larger interlayer distances (1.36 nm at room temperature and 1.08 nm at 98 °C) than those of graphene oxide (0.87 nm) and graphite (0.34 nm). According to the overall oxygen analysis data, the reduction process at 98 °C was more efficient than that of room temperature: however the epoxy- and carboxylic groups were completely removed at both temperatures.

Index Terms— Graphene-oxide; Reduced graphene-oxide; XPS; Raman.

I. INTRODUCTION

The use of graphene oxide as a material for the preparation of individual graphene sheets in bulk-quantity, has attracted great attention in recent years [1-3]. In addition, the incredibly large specific surface area, the abundant oxygen-containing surface functionalities (including epoxide, hydroxyl, carbonyl, and carboxylic groups) and the high water compatibility afford graphene oxide sheets of great promise for future applications [1,2]. For instance, graphene oxide nano-sheets modified with polyethylene glycol have been employed as aqueous compatible carriers for water-insoluble drug delivery [4]. The oxygen-containing functional groups on graphene oxide sheets have been used as sites for the deposition of metal nanoparticles and organic macromolecules, including porphyrins. This has opened up a novel route to a range of multifunctional-nanometer scaled catalytic, magnetic, and optoelectronic materials [5-7]. Graphene oxide sheets, with their distinctive nanostructure hold great promise for potential application in many technological fields that include nanoelectronics [8], sensors [9], nanocomposites [10], batteries [11], and capacitors [12]. A number of reports discussing the growth and exfoliation properties of graphene have appeared. One promising, low-cost, and easily up-scalable alternative to the use of graphene is to employ the product obtained on

reduction of graphite oxide [2,13,14], a layered material whose constituting graphene layers are functionalized with epoxy and hydroxyl groups and are easily exfoliated in water. The resulting graphene oxide monolayers can be deposited in controllable density onto a large variety of substrates, thus enabling the preparation of thin conductive films on both rigid and flexible substrates [1,15,16]. Although chemical reduction of close-to-insulating graphene oxide can increase its conductivity by up to 4 orders of magnitude [17-19], thus far attained conductivities of reduced graphene oxide still fall behind that of pristine graphene by a factor of 10-100 [3,20]. There is general consensus that the inferior electrical performance of reduced graphene oxide originates from the presence of residual functional groups remaining after reduction. However, despite numerous spectroscopic [21-26] and microscopic [19,27,28] studies performed on both graphene oxide and reduced graphene oxide, the dependence of reduced graphene oxide on the reduction temperature has not yet been elucidated. We herein report an investigation of the effect of temperature on the preparation of the reduced graphene oxide.

II. EXPERIMENTAL SECTION

A. Preparation of Graphene Oxide.

The graphene oxide was prepared according to modified Hummers method [29,30] by reacting commercial flakes graphite powder (Aldrich) (5 g) and NaNO₃ (3.75 g) with conc. H₂SO₄ (375 mL). This mixture was stirred in an ice-water bath, and 22.5 g of KMnO₄ was slowly added over 1 h and stirring was continued for 2 h in an ice-water bath. After the mixture was stirred vigorously for 2 days at room temperature, 700 mL of 5 wt% H₂SO₄ aqueous solution was added over 1 h with stirring, and the temperature was kept at 98 °C. The resultant mixture was further stirred for 2 h at 98 °C. After the temperature was reduced to 60 °C, 15 mL of H₂O₂ (30 wt% aqueous solution) was added, and the mixture was stirred for 2 h at room temperature. To remove extraneous products from the oxidation (and any other inorganic impurities), the resultant mixture was purified by repeating the following procedure cycle 20 times: centrifugation, removal of the supernatant liquid, then dispersing the solid using vigorous stirring and bath ultrasonication for 1 h at a power of 150 W. The resultant solid was recovered by centrifugation, washed with deionized water and ethanol until H⁺ free, and then dried in air at 40 °C.

B. Reduction of Graphene Oxide with Hydrazine.

The graphene oxide (100 mg) prepared was loaded in a 250 mL round bottom flask and water (100 mL) was then added,

Kyeong-Won Park, Department of Chemistry and Research Institute of Natural Science, Gyeongsang National University, Jinju 660-701, Republic of Korea

yielding an inhomogeneous yellow-brown dispersion. This dispersion was sonicated using an ultrasonic bath cleaner (150 W) until it became clear with no visible particulate matter. In next step, the graphene oxide was reduced with hydrazine at room temperature and 98 °C. First, hydrazine hydrate (1.0 mL, 32.1 mmol) was added and the solution was stirred for 24 h at room temperature, during which time the reduced graphene oxide gradually precipitated as a black solid. In case of the high temperature reduction, hydrazine hydrate (1.0 mL, 32.1 mmol) was added and the clear solution was heated in an oil bath at 98 °C under a water-cooled condenser for 24 h over which time reduced graphene oxide gradually precipitated as a black solid. In both cases, the solid precipitates were recovered by centrifugation, washed with deionized water and ethanol until hydrazine free, and then dried in air at 40 °C.

C. Characterization of Graphite, Graphene Oxide and Reduced Graphene Oxide.

The powder X-ray diffraction (XRD) measurements of the samples were recorded on a Bruker D8-Advance X-ray powder diffractometer using Cu K α radiation ($\lambda = 0.1542$ nm) with scattering angles (2θ) of 5–80°, operating at 40 keV, cathode current of 20 mA. Scanning electron micrographs (SEM) were obtained from a JEOL JSM-840A scanning electron microscope. Transmission electron micrographs (TEM) were obtained with a JEOL JEM-200 CX transmission electron microscope operating at 200 kV. AFM images were taken on an AutoProbe CP/MT scanning probe microscope (XE-100(PSIA)). Imaging was carried out in non-contact mode using a V-shaped ‘Ultralever’ probe B (Park Scientific Instruments, borondoped Si with frequency $f_c = 78.6$ kHz, spring constants $k = 2.0$ -3.8 Nm $^{-1}$, and nominal tip radius 10 nm). All images were collected under ambient conditions at 50% relative humidity and 23 °C with a scanning raster rate of 1 Hz. Samples for AFM images were prepared by depositing dispersions of graphene oxide in ethanol on a freshly cleaved mica surface (Ted Pella Inc. Prod No. 50) and allowing them to dry in air. X-ray photoemission spectroscopy (XPS) measurements were performed using an ESCA-2000 (VG Microtech, UK) with a twin anode X-ray source (Mg/Al). Raman spectra were obtained using a Jobin Yvon/Horiba LabRAM spectrometer equipped with an integral microscope (Olympus BX 41). The 514.5 nm Ar-laser was used as an excitation source. Samples were sonicated in ethanol and drops were applied to a glass slide for observation. The sample was viewed using a green laser apparatus under a maximum magnification of $\times 50$, and a red laser apparatus under a magnification of $\times 100$. The FT-IR spectra were recorded on a Bruker VERTEX 80v model using a KBr disk method.

III. RESULTS AND DISCUSSIONS

The graphene oxide was prepared from flakes graphite by modified Hummers method [29,30] and reduced graphene oxide was prepared by reduction of graphene oxide with hydrazine at room temperature and 98 °C. SEM and TEM images of graphite, graphene oxide, and reduced graphene

oxide are shown in Fig. 1. Compared with graphite (Fig. 1a), the general structure of graphene oxide (Fig. 1b) is greatly changed. It is found that the jeep-shaped graphene oxide thin plates are well exfoliated. As shown in Fig. 1d, it also can be seen from the typical TEM image of graphene oxide that it was fully exfoliated into nanosized sheets with micrometer-long wrinkles by ultrasonic treatment, illustrating clearly the flake-shaped graphene oxide sheets. These platelets are attributed to reduced graphene oxide (Fig. 1c) caused by the reduction of graphene oxide surface using hydrazine. Accordingly, the SEM image of reduced graphene oxide (Fig. 1c) is similar to that of original graphite, but each sheet of reduced graphene oxide has grown much bigger than that of the original graphite image.

Furthermore, AFM images (Fig. 2) provide morphological information about the graphene oxide. Sonication treatment of the graphene oxide truncated it from several hundreds of nanometers to less than 100 nm in lateral width, while the thickness remained unaltered at 1-2 nm, as revealed by the AFM images. Comparing this result with previous in the literature [1,13,30,31], we confirmed that the graphene oxide prepared in this work has the characteristic of single or two layered sheets.

To characterize the structures of the graphene oxides upon reduction, the XRD patterns were obtained. The XRD patterns shown in Fig. 3 reveal that the (C110) diffraction peak of graphite (Fig. 3a) appears at 26.8°, which means the interlayer space is 0.34 nm. After the exfoliation, the interlayer space of the resulting graphene oxide (Fig. 3b; 10.1°, 0.87 nm) became greater than that of graphite as a result of the introduction of oxygenated functional groups on the graphene sheets [31-33]. The XRD patterns for reduced graphene oxides prepared at room temperature (Fig. 3c; 7.01°, 1.36 nm) and 98 °C (Fig. 3d; 8.59°, 1.05 nm) exhibit commonly the main peak 24.3°. The main peak appears more predominantly at room temperature, indicating that some additional peaks observed for the sample prepared at 98 °C are originated to the structural deformation which occurs on decomposition of the epoxy groups into hydroxyl and carboxylic groups. Consequently, it was found that the reduction accomplished at 98 °C is more efficient than that did at room temperature. Raman spectroscopy can be employed to characterize the bonding, ordering, and crystallite size in carbon materials. It is well known that the Raman band at around 1582 cm $^{-1}$ (the G-band) is due to the in-plane phonon modes of graphene, which indicates sp 2 bonding. Also, the band at around 1353 cm $^{-1}$ is due to disorder in the graphene layers caused by sp 3 bonding (the D-band) [34]. Fig. 4 shows the Raman spectra of graphite, graphene oxide, and reduced graphene oxide (room temperature and 98 °C): the two peaks appeared ca. 1350 and 1590 cm $^{-1}$ correspond to the D and G bands, respectively. The Raman spectrum of graphite in (Fig. 4a) shows the in-phase vibration of the graphite lattice at 1592 cm $^{-1}$ (G band) and a weak D band at 1351 cm $^{-1}$ [34,35], indicating its well-ordered structure. In the Raman spectrum of graphene oxide (Fig. 4b), the G band is broadened and shifts to higher frequency (1593 cm $^{-1}$) due to the presence of isolated double bonds that resonate at higher frequencies than the G band of graphite [24].

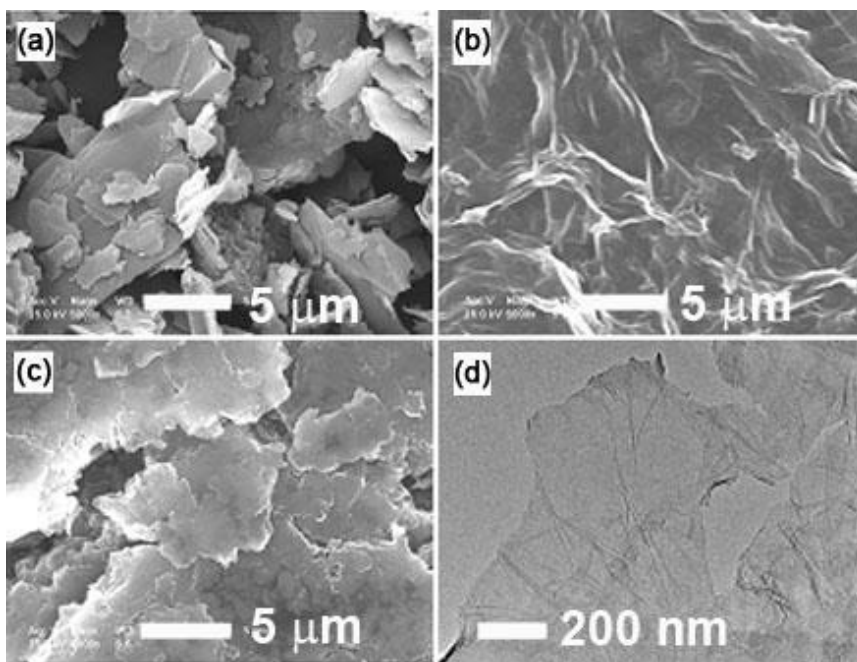


Fig. 1. SEM image of (a) graphite, (b) graphene oxide, (c) reduced graphene oxide at 98 °C, and (d) TEM image of graphene oxide.

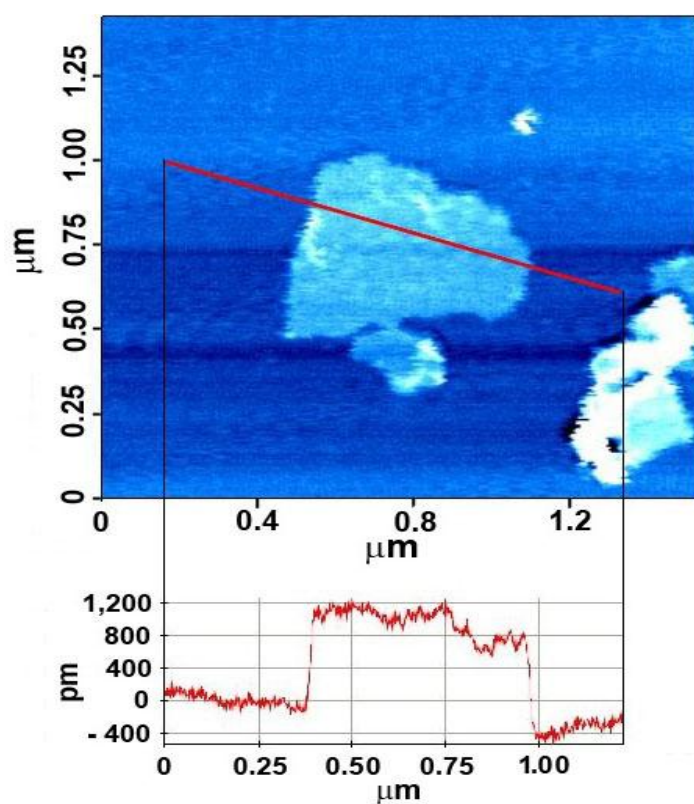


Fig. 2. AFM image of graphene oxide.

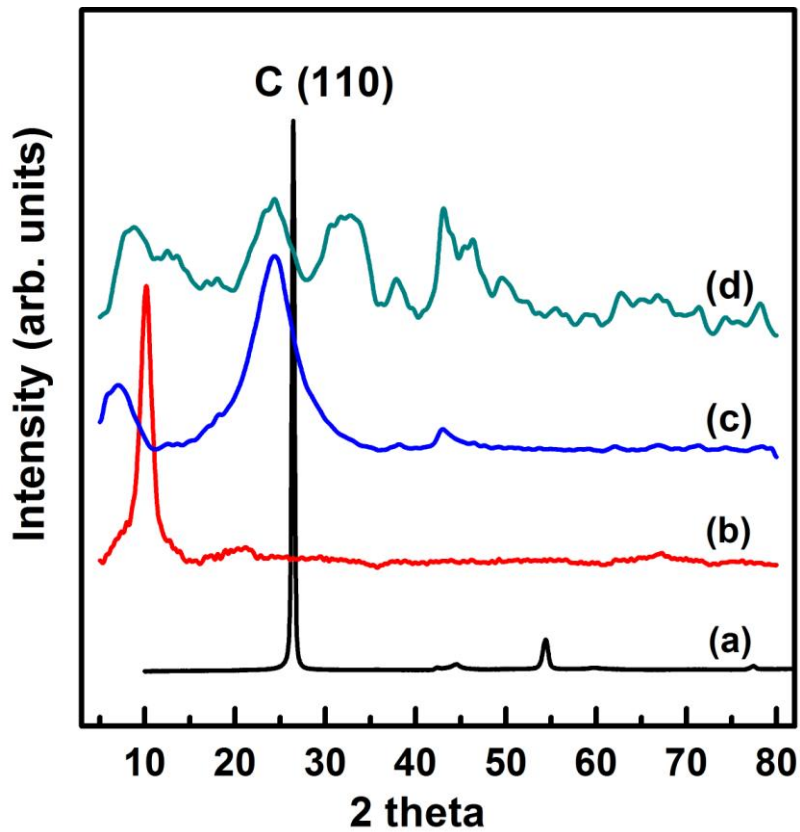


Fig. 3. XRD patterns of (a) graphite, (b) graphene oxide, (c) reduced graphene oxide at room temperature, and (d) reduced graphene oxide at 98 °C.

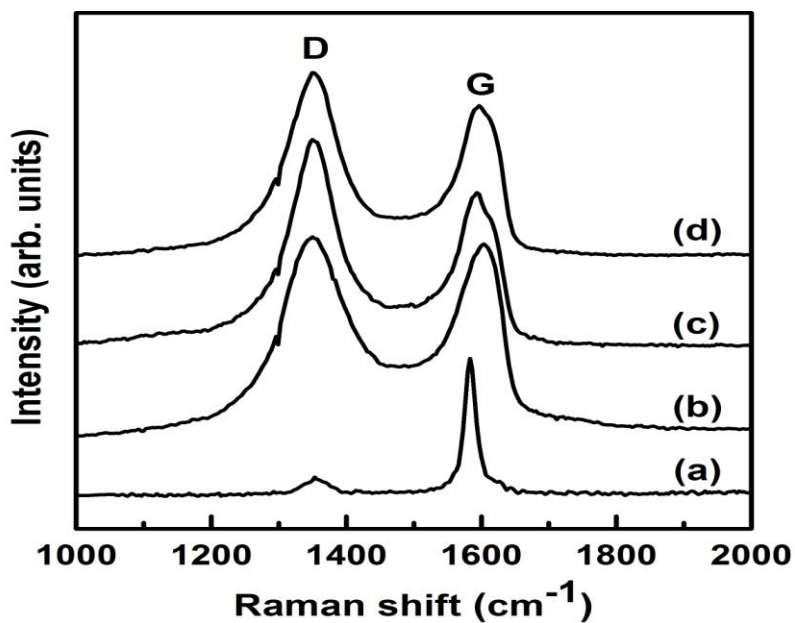


Fig. 4. Raman spectra of (a) graphite, (b) graphene oxide, and (c) and (d) reduced graphene oxides at (c) room temperature, and (d) 98 °C.

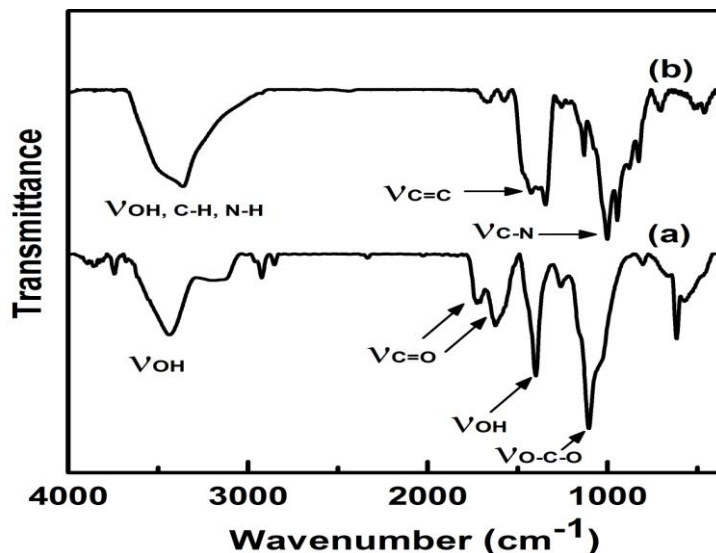


Fig. 5. FT-IR spectra of (a) graphene oxide and (b) reduced graphene oxide at 98 °C.

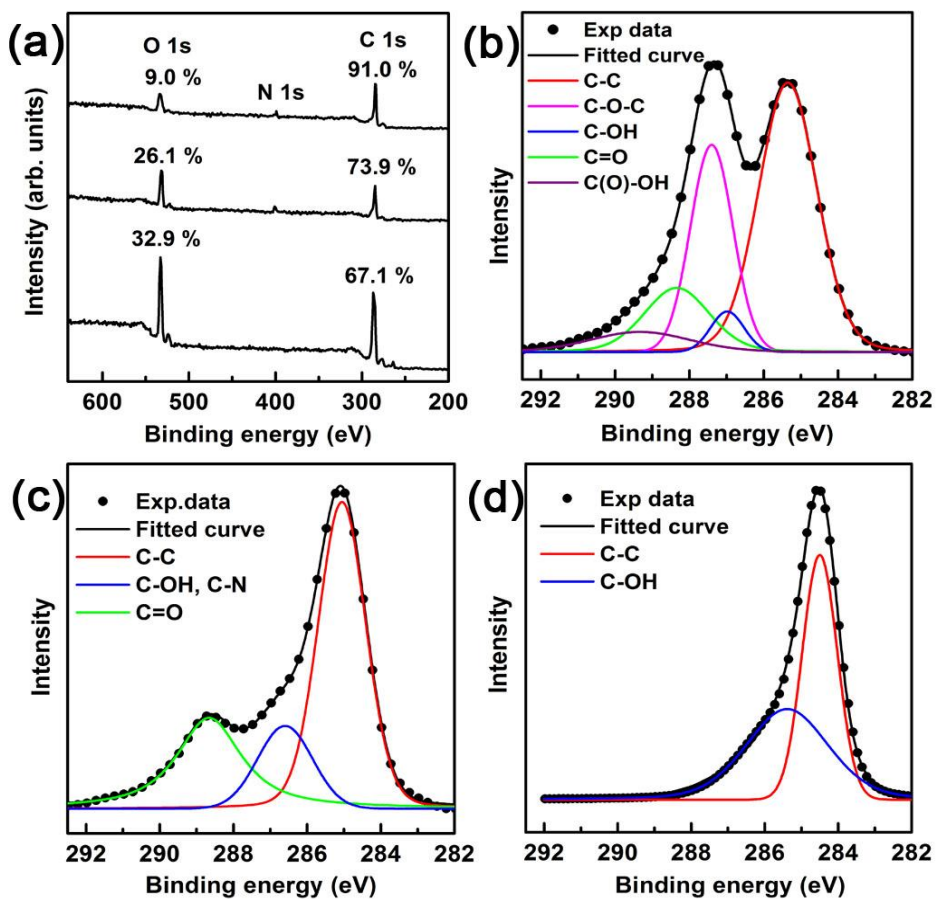


Fig. 6. XPS analysis: (a) wide scan for (bottom) graphene oxide, (middle) reduced graphene oxide at room temperature, (top) reduced graphene oxide at 98 °C, (b) graphene oxide in C 1s region, and (c and d) reduced graphene oxide at (c) room temperature C 1s region, and (d) 98 °C C 1s region.

Table 1: XPS peak locations and relative areas for graphene oxide and reduced graphene oxide

		Graphene oxide		Reduced graphene oxide (treated with N ₂ H ₄ for 24 h)			
				RT		98 °C	
		BE ^a	Relative	BE ^a	Relative	BE ^a	Relative
		(eV)	area (%)	(eV)	area (%)	(eV)	area (%)
	C-C	285.35	49.58	285.10	54.80	284.53	83.94
	C-OH	286.98	4.04	286.60	15.94	285.66	11.57
Functional group	C-O-C	287.40	26.37	287.40	0	287.40	0
	C=O	288.34	13.54	288.66	29.26	286.55	4.48
	C(O)-OH	289.33	6.46	289.33	0	289.33	0
Abundant ^b ratio	C		1		1		1
	O		0.50		0.35		0.09

^a Binding energy. ^bOxygen contents are normalized by each carbon content value.

In addition, the D band at 1339 cm⁻¹ becomes prominent, indicating the decrease in size of the in-plane sp² domains (G band) due to the extensive oxidation during exfoliation. Upon hydrazine reduction at two different temperatures, both of the Raman spectra for reduced graphene oxides also exhibit D and G bands (Fig. 3c and 3d). Notably, the increase in the D/G intensity ratios for reduced graphene oxides, compared to graphene oxide, indicates a decrease in the size of the in-plane sp² domains and, in same time, an increase of the areas with disordered structure upon reduction [36].

To characterize the oxygenated functional groups on the graphene oxides upon reduction, the FT-IR spectra were obtained. Fig. 5a displays the characteristic peaks of the FT-IR spectra of graphene oxide: a broad band ranging from 3600 to 3250 cm⁻¹ indicates the presence of -OH group, the stretching vibration for C=O from the carboxylic groups at 1712 cm⁻¹, the stretching vibrations of C-O from ether group at 1055 cm⁻¹, the in-plane OH bending mode [37] at 1349 cm⁻¹, and the C=C aromatic ring stretching peak at 1570 cm⁻¹. According to the FT-IR spectra, it was found that the graphene oxide contains diverse types of the oxide forms such as hydroxy, carbonyl, carboxylic, and epoxy groups.

After treatment of graphene oxide with hydrazine, as shown in Fig. 5b, the characteristic vibration bands of oxide groups (ν_{C=O}, ν_{O-C-O} and ν_{C-OH}) decreased dramatically, indicating that graphene oxide was reduced efficiently. New peaks at 1005 and 671 cm⁻¹ due to ν_{C-N} and δ_{a(N-H)}, respectively, in the spectrum of reduced graphene oxide at 98 °C also indicate the presence of the C-N bonding produced by the by-reaction with hydrazine at the higher temperature.

We have also investigated an amount of oxygen and elemental for graphene oxide and reduced graphene oxide by XPS. In the XPS wide scan analysis (Fig. 6a), the peaks at 284.2, 533.5, and 399.6 eV correspond to C (1s of sp²), O (1s of graphene oxide, reduced graphene oxide), and N (1s of the nitrogen doped from hydrazine), respectively. Comparing the oxygen levels of the samples, we found that the oxygen levels of in reduced graphene oxides (26% at room temperature and 9% at 98 °C) were much lower than that in graphene oxide (33%), indicate an obvious reduction. Furthermore, once again, this indicates more effective reduction effect at high temperature than that at room temperature. The related experimental results are also summarized in Table 1.

The C 1s peak in graphene oxide (Fig. 6b) indicates a considerable degree of oxidation with five components that correspond to carbon atoms in different functional groups [38]: C in non-oxygenated ring (284.8 eV), C in C-O bonds (286.2 eV), C in carbonyl (287.9 eV), C in C-OH groups (286.6 eV), and C in carboxylate (289.0 eV) [38]. Meanwhile, the C1s peak for the reduced graphene oxide treated at room temperature (Fig. 6c) exhibits the intensities of all C 1s peaks of the carbon binding to oxygen, especially the peak of carbon bonded oxygen, decreased dramatically, indicating that most of the oxygen-containing functional groups were removed after being reduced during 24 h at room temperature. The XPS spectra for the reduced graphene oxide treated at 98 °C (Fig. 6d) indicate that most of the oxygen-containing functional groups were removed on reduction at 98 °C. This result also shows that the oxygen-containing functional groups completely disappeared

except the partially remaining -OH and C=N (285.9 eV) [39].

IV. CONCLUSIONS

The diverse types of oxides for the graphite and the graphene oxides before and after reduction with hydrazine at different temperatures have been analyzed. We found that the reduction process carried out at 98 °C is more efficient to remove the oxides than that did at room temperature. Epoxy- and carboxylic groups, however, were completely removed at both temperatures. We believe that these results can serve the fundamental information to the chemical and physical modifications of graphenes.

REFERENCES

- [1] D. Li, M. B. Müller, S. Gilje, R. B. Kaner, G. G. Wallace, *Nature Nanotechnol.* 3 (2008) 101-105.
- [2] S. Park, R. S. Ruoff, *Nature Nanotechnol.* 4 (2009) 217-223.
- [3] V. C. Tung, M. J. Allen, Y. Yang, R. B. Kaner, *Nature Nanotechnol.* 4 (2009) 25-29.
- [4] Z. Liu, J. T. Robinson, X. Sun, H. Dai, *J. Am. Chem. Soc.* 130 (2008) 10876-10877.
- [5] J. R. Lomeda, C. D. Doyle, D. V. Kosynkin, W. Hwang, J. M. Tour, *J. Am. Chem. Soc.* 130 (2008) 16201-16206.
- [6] R. Muszynski, B. Seger, P. V. Kamat, *J. Phys. Chem. C* 112 (2008) 5263-5266.
- [7] Y. Xu, Z. Liu, X. Zhang, Y. Wang, J. Tian, Y. Huang, Y. Ma, X. Zhang, Y. Chen, *Adv. Mater.* 21 (2009) 1275-1278.
- [8] Y. Sui, J. Appenzeller, *Nano Lett.* 9 (2009) 2973-2973.
- [9] C. S. Shan, H. F. Yang, J. F. Song, D. X. Han, A. Ivaska, L. Niu, *Anal. Chem.* 81 (2009) 2378-2382.
- [10] D. W. Wang, F. Li, J. P. Zhao, W. C. Ren, Z. G. Chen, J. Tan, Z. S. Wu, I. Gentle, G. Q. Lu, H. M. Cheng, *ACS Nano* 3 (2009) 1745-1750.
- [11] P. Guo, H. H. Song, X. H. Chen, *Electrochem. Commun.* 11 (2009) 1320-1324.
- [12] Y. Wang, Z. Q. Shi, Y. Huang, Y. F. Ma, C. Y. Wang, M. M. Chen, Y. S. Chen, *J. Phys. Chem. C* 113 (2009) 13103-13107.
- [13] S. Stankovich, D. A. Dikin, G. H. B. Dommett, K. M. Kohlhaas, E. J. Zimney, E. A. Stach, R. D. Piner, S. T. Nguyen, R. S. Ruoff, *Nature* 442 (2006) 282-286.
- [14] S. Stankovich, R. D. Piner, X. Q. Chen, N. Q. Wu, S. T. Nguyen, R. S. Ruoff, *J. Mater. Chem.* 16 (2006) 155-158.
- [15] X. Wang, L. J. Zhi, K. Mullen, *Nano Lett.* 8 (2008) 323-327.
- [16] G. Eda, G. Fanchini, M. Chhowalla, *Nature Nanotechnol.* 3 (2008) 270-274.
- [17] I. Jung, D. A. Dikin, R. D. Piner, R. S. Ruoff, *Nano Lett.* 8 (2008) 4283-4287.
- [18] S. Gilje, S. Han, W. Minsheng, L. W. Kang, R. B. Kaner, *Nano Lett.* 7 (2007) 3394-3398.
- [19] C. Gómez-Navarro, R. T. Weitz, A. M. Bittner, M. Scolari, A. Mews, M. Burghard, K. Kern, *Nano Lett.* 7 (2007) 3499-3503.
- [20] V. López, R. S. Sundaram, C. Gómez-Navarro, D. Olea, M. Burghard, J. Gómez-Herrero, F. Zamora, K. Kern, *Adv. Mater.* 21 (2009) 4683-4687.
- [21] T. Szabo, O. Berkesi, P. Forgo, K. Josepovits, Y. Sanakis, D. Petridis, I. Dekany, *Chem. Mater.* 18 (2006) 2740-2749.
- [22] W. W. Cai, R. D. Piner, F. J. Stadermann, S. Park, M. A. Shaibat, Y. Ishii, D. X. Yang, A. Velamakanni, S. J. An, M. Stoller, J. H. An, D. M. Chen, R. S. Ruoff, *Science* 321 (2008) 1815-1817.
- [23] A. Lerf, H. Y. He, M. Forster, J. Klinowski, *J. Phys. Chem. B* 102 (1998) 4477-4482.
- [24] K. N. Kudin, B. Ozbas, H. C. Schniepp, R. K. Prud'homme, I. A. Aksay, R. Car, *Nano Lett.* 8 (2008) 36-41.
- [25] C. Mattevi, G. Eda, S. Agnoli, S. Miller, K. A. Mkhoyan, O. Celik, D. Mastrogianni, G. Granozzi, E. Garfunkel, M. Chhowalla, *Adv. Funct. Mater.* 19 (2009), 2577-2583.
- [26] A. Bagri, C. Mattevi, M. Acik, Y. J. Chabal, M. Chhowalla and V. B. Shenoy, *Nature Chemistry* 2 (2010), 581-587.
- [27] D. Pandey, R. Reifengerger, R. Piner, *Surf. Sci.* 602 (2008) 1607-1613.
- [28] K. A. Mkhoyan, A. W. Contryman, J. Silcox, D. A. Stewart, G. Eda, C. Mattevi, S. Miller, M. Chhowalla, *Nano Lett.* 9 (2009) 1058-1063.
- [29] W. Hummers, R. Offeman, *J. Am. Chem. Soc.* 80 (1958) 1339-1340.
- [30] S. Donner, H. W. Li, E. S. Yeung, M. D. Porter, *Anal. Chem.* 78 (2006) 2816-2822.
- [31] H. K. Jeong, Y. P. Lee, R. J. W. E. Lahaye, M. H. Park, K. H. An, I. J. Kim, C. W. Yang, C. Y. Park, R. S. Ruoff, Y. H. Lee, *J. Am. Chem. Soc.* 130 (2008) 1362-1366.
- [32] C. Xu, X. Wang, J. Zhu, *J. Phys. Chem. C* 112 (2008) 19841-19845.
- [33] A. B. Bourlinos, D. Gournis, D. Petridis, T. Szabo, A. Szeri, I. Dekany, *Langmuir* 19 (2003) 6050-6055.
- [34] A. C. Ferrari, J. C. Meyer, V. Scardaci, C. Casiraghi, M. Lazzeri, F. Mauri, S. Piscanec, D. Jiang, K. S. Novoselov, S. Roth, *Phys. Rev. Lett.* 97 (2006) 187401-187404.
- [35] F. Tuinstra, J. L. Koenig, *J. Chem. Phys.* 53 (1970) 1126-1130.
- [36] A. C. Ferrari, J. Robertson, *Phys. Rev. B* 61 (2000) 14095-14107.
- [37] L. J. Bellamy, *The Infrared Spectra of Complex Molecules*, Chapman and Hall, London 1975.
- [38] D. Briggs, G. Beamson, *High Resolution XPS of Organic Polymers: The Scienta ESCA300 Database*, John Wiley & Sons Inc, New York, 1992, P. 266.
- [39] R. J. Waltman, J. Pacansky, C. W. Bates., Jr. *Chem. Mater.* 5 (1993) 1799-1804.